

การประเมินขนาดของแรงและรูปแบบสำหรับการ การดันเข้าฟันกรามแท้บนซี่ที่หนึ่ง ด้วยหลักยึดหมุด ฝังในกระดูกวิเคราะห์โดยวิธีไฟไนต์เอลิเมนต์ Evaluation of the Magnitudes of Force and Patterns for the Intrusion of Maxillary First Molar Teeth with Mini-Screw Anchorage, Analyzed Using the Finite Element Method

ปาณิศา พีระณิขกุล¹, วิรัช พัฒนาการณ์², ชาย รังสิยากุล³

¹คลินิกเอกซน กรุงเทพมหานคร

²ภาควิชาทันตกรรมจัดฟันและทันตกรรมสำหรับเด็ก คณะทันตแพทยศาสตร์ มหาวิทยาลัยเชียงใหม่

³ภาควิชาวิศวกรรมเครื่องกล คณะวิศวกรรมศาสตร์ มหาวิทยาลัยเชียงใหม่

Phanisa Pheerawanitchakun¹, Virush Patanaporn², Chaiy Rungsiyakul³

¹Private Practice, Bangkok, Thailand

²Department of Orthodontics and Pediatric Dentistry, Faculty of Dentistry, Chiang Mai University

³Department of Mechanical Engineering, Faculty of Engineering, Chiang Mai University

ชม. ทันตสาร 2561; 39(1) : 95-111

CM Dent J 2018; 39(1) : 95-111

บทคัดย่อ

การศึกษานี้มีวัตถุประสงค์เพื่อประเมินขนาดของแรงที่มากที่สุดสำหรับการดันเข้าฟันกรามแท้บนซี่ที่หนึ่ง โดยไม่เกินความดันหลอดเลือดฝอยในเอ็นยึดปริทันต์ (0.0047 เมกะพาสคัล) และเพื่อหารูปแบบของแรงที่เหมาะสมเมื่อเปรียบเทียบรูปแบบสองแบบสำหรับการดันเข้าฟันกรามแท้บนซี่ที่หนึ่ง ระหว่างรูปแบบที่ใช้หลักยึดหมุดฝังในกระดูก 2 ตัว และ 3 ตัว วิเคราะห์โดยวิธีไฟไนต์เอลิเมนต์ แบบจำลองไฟไนต์เอลิเมนต์สามมิติถูกสร้างด้วยโปรแกรมโซลิดเวิร์คส์ กำหนดให้แรงดันเข้ากระทำที่กึ่งกลาง

Abstract

The purposes of this study were to evaluate the greatest magnitude of force that can be applied in order to initiate the intrusion of maxillary first molar teeth without exceeding the periodontal capillary-vessel blood pressure of 0.0047 MPa and to compare the use of anchorage from either two or three mini-screws to determine the optimal pattern of force for the intrusion of maxillary first molar teeth, using the finite element method. A three-dimensional finite

Corresponding Author:

วิรัช พัฒนาการณ์

ศาสตราจารย์คลินิก ทันตแพทย์ ภาควิชาทันตกรรมจัดฟันและทันตกรรมสำหรับเด็ก คณะทันตแพทยศาสตร์ มหาวิทยาลัยเชียงใหม่

Virush Patanaporn

Clinical Professor, Department of Orthodontics and Pediatric Dentistry, Faculty of Dentistry, Chiang Mai University, Chiang Mai, 50200, Thailand

E-mail: vr167420@hotmail.com

ด้านบดเคี้ยวของฟันกรามแท้บนซี่ที่หนึ่ง และหาขนาดของแรงที่มากที่สุดจากการให้แรงในปริมาณต่าง ๆ กัน ในการหาแนวแรงที่เหมาะสมทั้งสองรูปแบบ ทำโดยการเปรียบเทียบความแตกต่างของรูปแบบการกระจายความเค้นในเอ็นยึดปริทันต์ รวมถึงลักษณะการเคลื่อนที่เริ่มต้นของการดันเข้าฟันกรามแท้บนซี่ที่หนึ่ง ที่เกิดขึ้นจากการใช้แรงปริมาณที่คำนวณได้กระทำต่อตัวฟันในตำแหน่งต่างกันจากการใช้หลักยึดหมุดฝังในกระดูก 2 ตัว และ 3 ตัว โดยใช้โปรแกรมออบาคัส รูปแบบที่ใช้หลักยึดหมุดฝังในกระดูก 2 ตัว หมุดที่วางทางด้านแก้มจะวางในตำแหน่งระหว่างรากของฟันกรามแท้ซี่ที่หนึ่งและสอง หมุดที่วางทางด้านเพดานจะวางในตำแหน่งระหว่างรากของฟันกรามน้อยแท้ซี่ที่สอง และฟันกรามแท้ซี่ที่หนึ่ง ในขณะที่รูปแบบที่ใช้หลักยึดหมุดฝังในกระดูก 3 ตัว หมุด 2 ตัวที่วางด้านแก้ม จะวางในตำแหน่งระหว่างรากของฟันกรามน้อยแท้ซี่ที่สอง และฟันกรามซี่ที่หนึ่ง และระหว่างรากของฟันกรามแท้ซี่ที่หนึ่ง และ สองตามลำดับ หมุดที่วางทางด้านเพดานจะวางในตำแหน่งรอยประสานกระดูกกลางเพดาน จากการศึกษาพบว่า ขนาดของแรงที่มากที่สุดสำหรับการดันเข้าฟันกรามแท้บนซี่ที่หนึ่ง มีค่าเท่ากับ 13 กรัม และพบว่ารูปแบบที่ใช้หลักยึดหมุดฝังในกระดูก 2 ตัว เป็นรูปแบบที่เหมาะสมสำหรับการดันเข้าฟันกรามแท้บนซี่ที่หนึ่ง เนื่องจาก ทำให้เกิดการเคลื่อนมาทั้งส่วนรากฟันและตัวฟันพร้อม ๆ กัน มากกว่ารูปแบบที่ใช้หลักยึดหมุดฝังในกระดูก 3 ตัว

element model was constructed using SolidWorks software. Intrusive force was applied at the middle of the occlusal surface of the maxillary first molar tooth. The finite element model was able to determine the greatest magnitude of force applied by simulation of various force magnitudes. To determine the optimal pattern of force, the different patterns of stress distribution and initial displacements of maxillary first molar teeth between the pattern of intrusion using two and three mini-screws were compared using ABAQUS software. In the pattern of intrusion using two mini-screws, on the buccal side, a mini-screw was placed between the roots of the first and second molar teeth. On the palatal side, a mini-screw was placed between the roots of the second premolar and first molar teeth. In the pattern of intrusion using three mini-screws, two mini-screws were inserted into the maxillary buccal alveolar bone, one between the roots of the second premolar and first molar teeth and the other between the roots of the first and second molar teeth. The third mini-screw, in the mid-palatal suture, supplied the palatal anchorage. In the case of each pattern, the calculated magnitude of forces was applied to each maxillary first molar tooth. Results showed that the greatest magnitude of force for the intrusion of maxillary first molar teeth was 13 grams. It was concluded that the pattern with two mini-screws was the optimal pattern of force for the intrusion of the maxillary first molar because this pattern provided more bodily movement than that with three mini-screws.

คำสำคัญ: การดันเข้าฟันกรามแท้บนซี่ที่หนึ่ง หมุดฝังในกระดูก วิธีไฟไนต์เอลิเมนต์

Keywords: intrusion of maxillary first molar teeth, mini-screw anchorage, finite element method

Introduction

A supra-erupted molar is one of the most common clinical findings in adult patients. Delayed replacement of lost teeth often leads to extrusion of the opposing teeth into the edentulous space, leading to masticatory insufficiency, periodontal problems and temporomandibular disorders. When a prosthesis is planned for the edentulous area, re-establishing a functional posterior occlusion requires a comprehensive dental treatment plan. If the dental alveolar extrusion is mild, it is possible to gain the space by performing coronoplasty and endodontic treatment of the supraerupted tooth. When the extrusion is moderate, orthodontic intrusion is recommended.

Intrusion is associated with numerous side effects from the periodontium and cementum.⁽¹⁾ However, in recent years, successful orthodontic intrusion has been clinically documented and is considered a safe procedure. The magnitude and direction of forces are carefully monitored.⁽²⁾ In the literature, intrusive force values vary among authors from 50 to 500 grams.⁽³⁻⁷⁾ This variation may be explained by the difficulty in measuring the force applied by complex biomechanical systems using continuous straight archwires,⁽⁸⁾ the difference in root surface area of each tooth as well as the differences among various techniques. Generally, heavier forces should be avoided, given the fact that in this type of movement the force is distributed over a small area around the apex.⁽⁹⁾ Due to stress concentration over a limited area, orthodontic intrusion is considered to present risks for root resorption of involved teeth. The recommended force for miniscrew-supported maxillary molar intrusion is 100 to 200 grams.⁽¹⁰⁾ However, there is no agreement on the proper load for molar intrusion.

To intrude supra-erupted maxillary molars, orthodontic anchorage can be prepared by incorporating multiple teeth, combined with extra-oral headgear, or using mini-plates as bony anchorage. Nowadays, orthodontic intrusion has gained wide acceptance because the use of orthodontic temporary anchorage devices (TADs) can be a simple treatment that does not require other teeth or additional extra-oral anchorage.^(5,11) The available literature for maxillary molar intrusion with skeletal anchorage devices, especially mini-screws, consists mainly of case reports.^(5,12-16) However, studies on biomechanical effects, such as stress and displacement on the tooth and the periodontal ligament, are limited. Because *in-vivo* studies are not quite sufficient in evaluating biomechanical effects, finite element analysis, a general method in engineering, has become a useful option for the assessment of biomechanical factors in orthodontics. The finite element method (FEM) is an accurate technique used to analyze structural stress. This method uses a computer to calculate large numbers of equations to identify the stress on the basis of the physical properties of the structures being analyzed.⁽¹⁷⁾ In orthodontics, the FEM provides the orthodontist with quantitative data that can provide the understanding of physiological reactions that happen within the dentoalveolar complex.

The main purpose of this study was to evaluate the greatest magnitude of force that can be applied in order to initiate the intrusion of maxillary first molar teeth without exceeding the periodontal capillary-vessel blood pressure⁽¹⁸⁾ of 0.0047MPa.⁽¹⁹⁾ The minor purpose was to compare the use of anchorage from either two or three mini-screws to determine the optimal pattern of force for the intrusion of maxillary first molar teeth, using the finite element method. The optimal pattern would be the one that produces bodily movement, rather than tipping, of the tooth.

Materials and Methods

Construction and Assembly of solid models

Commercial tooth models (Model-i21D-400G; Nissin Dental Products, Kyoto, Japan), which included the maxillary second premolar, first molar and second molar teeth, were scanned through the use of a 3-D scanner (D800 3D Scanner, 3 Shape, New Providence, New Jersey, USA) to produce the digital tooth images. These three maxillary posterior teeth were modeled manually, as suggested by Wheeler⁽²⁰⁾ to construct the three-dimensional tooth models according to the standard dimensions of human teeth.

The periodontal ligaments of the maxillary second premolar, first molar and second molar teeth were assumed to have a thickness of 0.2 mm, as previously described in another FEM study⁽²¹⁾ and to be constant all over the roots. They were constructed using Materialised 3-matic software (3-matic Research 9.0 software; Materialise, Leuven, Belgium). The maxillary model (cortical and cancellous bone) was established using a three-dimensional computer-aided design program (SolidWorks software, Dassault Systèmes Americas, Waltham, Mass, USA). Solid models, including the maxillary second premolar, first molar and second molar teeth, periodontal ligament (PDL) and the maxillary bone (cortical and cancellous bone), were assembled using SolidWorks. The maxillary posterior tooth roots were embedded in the maxillary model, which was programmed to trace the cemento-enamel junction's contour gingivally. The thickness of the cortical bone was assumed to be 2.0 mm. The posterior teeth from the second premolar to the second molar were leveled, and the maxillary first molar without its surrounding alveolar bone was extruded by 1.5 mm.

Finite element model construction

Following construction of the solid model, it was imported into ABAQUS software (Dassault Systèmes

Americas). The assembled model of a maxilla with maxillary posterior teeth was meshed into several small elements. Tetrahedron elements with high mesh quality were used for intrusion of the maxillary first molar tooth. The meshed model contained 197,772 nodes and 959,647 elements. Convergence tests were performed to determine the reliability of the solutions obtained from comparing the discretization of the elements.

The x, y and z axes of the three-dimensional finite element model represented the mesio-distal, the gingivo-occlusal and the bucco-palatal directions, respectively. Thus -x, -y and -z axes represented the mesial direction, the gingival direction and the palatal directions, respectively. All the nodes on the mesial and distal surfaces of the cortical bone were constrained in all directions to prevent displacements from loading. Contacts between the maxillary second premolar, maxillary first molar and maxillary second molar teeth were defined as frictionless surfaces. The contact constraints between these teeth and the periodontal ligament were set up with the "tie" feature of the software program, as well as those between the cancellous bone and the periodontal ligament and between the cancellous bone and the cortical bone.

All materials in the finite element analysis were assumed to be homogeneous and isotropic. The material properties for tooth and bone were taken from a previous FE study⁽²²⁾ (Table 1). The hyperelastic property of the PDL was taken into consideration in this investigation, and the strain energy potential function for the Ogden model can be expressed as

$$W = \sum_{i=1}^N \frac{2\mu_i}{\alpha_i} (\bar{\lambda}_1^{\alpha_i} + \bar{\lambda}_2^{\alpha_i} + \bar{\lambda}_3^{\alpha_i} - 3) + \sum_{i=1}^N \frac{1}{D_i} (J - 1)^{2i} \quad (1)$$

where W is strain energy function, λ_1 , λ_2 and λ_3 are the principle stretches, and J is the elastic volume ratio. μ_i is related to the initial shear modulus of the material; α_i and D_i are the parameters of the material.

$$\bar{\lambda}_i = J^{-1/3} \lambda_i, \bar{\lambda}_1 \bar{\lambda}_2 \bar{\lambda}_3 = 1 \quad (2)$$

The data from an uniaxial tension test for the periodontal ligament in a previous study⁽²³⁾ was applied to fit the third order Ogden model. The coefficients of the third order Ogden model⁽²⁴⁾ are shown in Table 2. The Poisson's ratio for the PDL was assumed to be 0.45.

ตารางที่ 1 ค่าพารามิเตอร์แสดงถึงสมบัติเชิงกลของฟัน กระดูกทึบ และกระดูกโปร่ง⁽²²⁾

Table 1 Parameters for the mechanical properties of tooth and of cortical and cancellous bone.⁽²²⁾

Material	Young's modulus (MPa)	Poisson's ratio
Cortical bone	13700	0.26
Cancellous bone	1370	0.30
Tooth	19613.3	0.15

ตารางที่ 2 ค่าสัมประสิทธิ์ของแบบจำลองออกเดนลำดับที่สาม⁽²⁴⁾

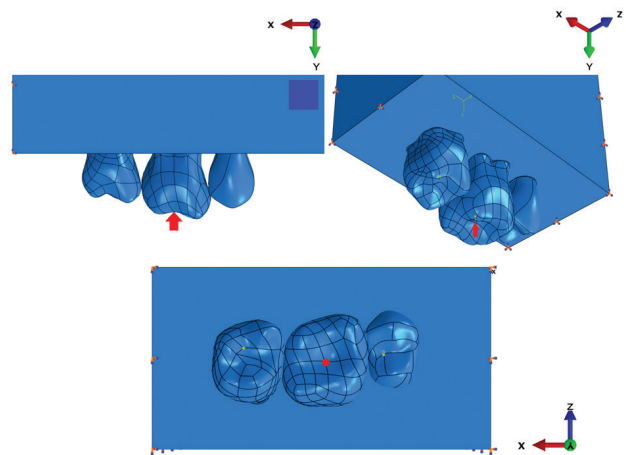
Table 2 Coefficients of the third order Ogden model.⁽²⁴⁾

i	μ_i	α_i	D_i
1	-24.4237016	1.99994222	4.87164332
2	15.8966494	3.99994113	0.00000000
3	8.56953079	-2.00005453	0.00000000

Definition of loading condition

First research hypothesis

To simulate maxillary first molar intrusion, intrusive force was applied at the middle of the occlusal surface of the maxillary first molar tooth. The force was transmitted through the center of resistance, parallel to the long axis of the maxillary first molar tooth (Figure 1). The finite element model was able to determine the greatest magnitude of force applied without exceeding the periodontal capillary-vessel blood pressure by simulation of various force magnitudes (5, 10, 11, 12, 13, 14, 15, 20, 25, 50, 100 g).



รูปที่ 1 แรงดันเข้าที่กึ่งกลางด้านบดเคี้ยวของฟันกรามแท้บนซี่ที่หนึ่ง (ลูกศรสีแดง)

Figure 1 Intrusive force at the middle of the occlusal surface of the maxillary first molar tooth (red arrow).

Second research hypothesis

When the various force magnitudes of intrusive force were applied (from the first research hypothesis), we found that the greatest magnitude of force without exceeding the periodontal capillary blood pressure of 0.0047 MPa was 13 g. In consequence, in the case of each pattern, finite element analysis was realized by applying a total of 13 g to each maxillary first molar tooth.

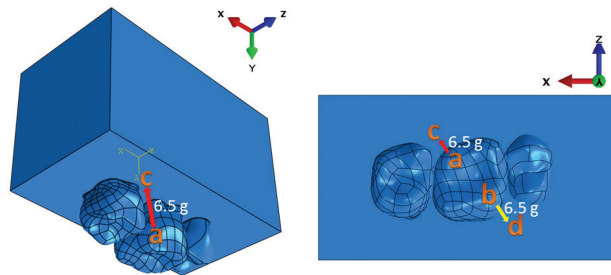
In the pattern of intrusion using two mini-screws, the finite element model was initiated with two force vectors: one at the distobuccal (Point a) and another at the mesiopalatal (Point b) angle of the maxillary first molar tooth. The force vectors were applied to the mini-screw positions on the buccal (Point c) and palatal (Point d) sides, respectively (Figure 2). Ultimately, Point c was located between the roots of the maxillary first and second molars teeth, whereas Point d was located between the roots of the maxillary second premolar and first molar teeth. In the vertical (occlusogingival) aspect, both positions were 6 mm apical to the CEJ. Lee *et al.*⁽²⁵⁾ and Garib *et al.*⁽²⁶⁾ found

that the mean thicknesses of the buccal and palatal bone plates of the maxillary first molar teeth 6 mm apically to the CEJ were 1.92 and 1.13 mm, respectively. As these thicknesses were applied to the buccopalatal positioning of the mini-screws, Point c and Point d were 1.92 and 1.13 mm away from the root surfaces, respectively. To simulate the maxillary first molar intrusion, 6.5 g of intrusive forces were applied on each side.

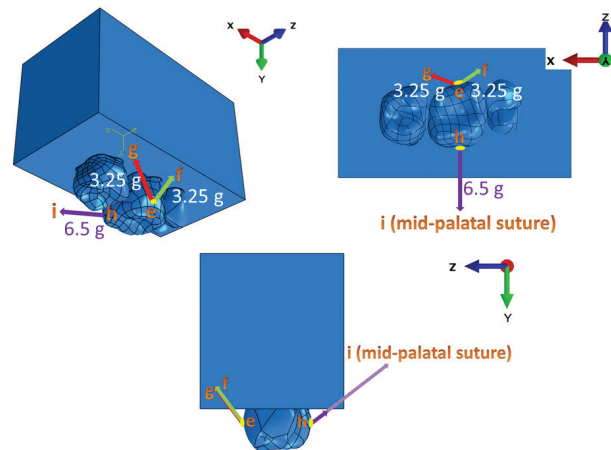
In the pattern of intrusion using three mini-screws, the finite element model was initiated with three force vectors (Figure 3). On the buccal side, the force vectors (Point e) were applied to the midpoint of the tooth. One force vector was directed to the mini-screw position between the roots of the maxillary second premolar and first molar, 6 mm apical to the CEJ (Point f). The other was directed between the roots of the maxillary first and second molar teeth, 6 mm apical to the CEJ (Point g). For the buccopalatal positioning of the mini-screws, both position were 1.92 mm⁽²⁵⁾ away from the root surface. On the palatal side, the force vector was applied to the midpoint of the palatal surface (Point h) and was directed towards Point i at the midpalatal suture (at the point where a perpendicular line from the central pit of the maxillary first molar teeth intersects the midpalatal suture). Moreover, the palatal force vector was angulated 45 degrees to the long axis of the maxillary first molar tooth.⁽²⁷⁾ Six point five grams of intrusive force were applied on the buccal side of the maxillary first molar, 3.25 g in the mesial and 3.25 g in the distal directions, whereas 6.5 g of intrusive force were applied perpendicularly on the palatal side.

The distribution and standard deviation of the von Mises stresses along the periodontal ligament and the initial tooth displacement measured at the four cusps and three root apices of the maxillary first molar tooth were analyzed. To determine tipping movements accurately, initial tooth displacements by comparing the same nodes, having the same coordinates in each

pattern at the root apices and the cusp tips, were evaluated by superimpositions of the tooth positions before and after force application.



รูปที่ 2 รูปแบบการดันเข้าด้วยหลักยึดหมุดฝังในกระดูก 2 ตัว
Figure 2 Pattern of intrusion using two mini-screws.



รูปที่ 3 รูปแบบการดันเข้าด้วยหลักยึดหมุดฝังในกระดูก 3 ตัว
Figure 3 Pattern of intrusion using three mini-screws.

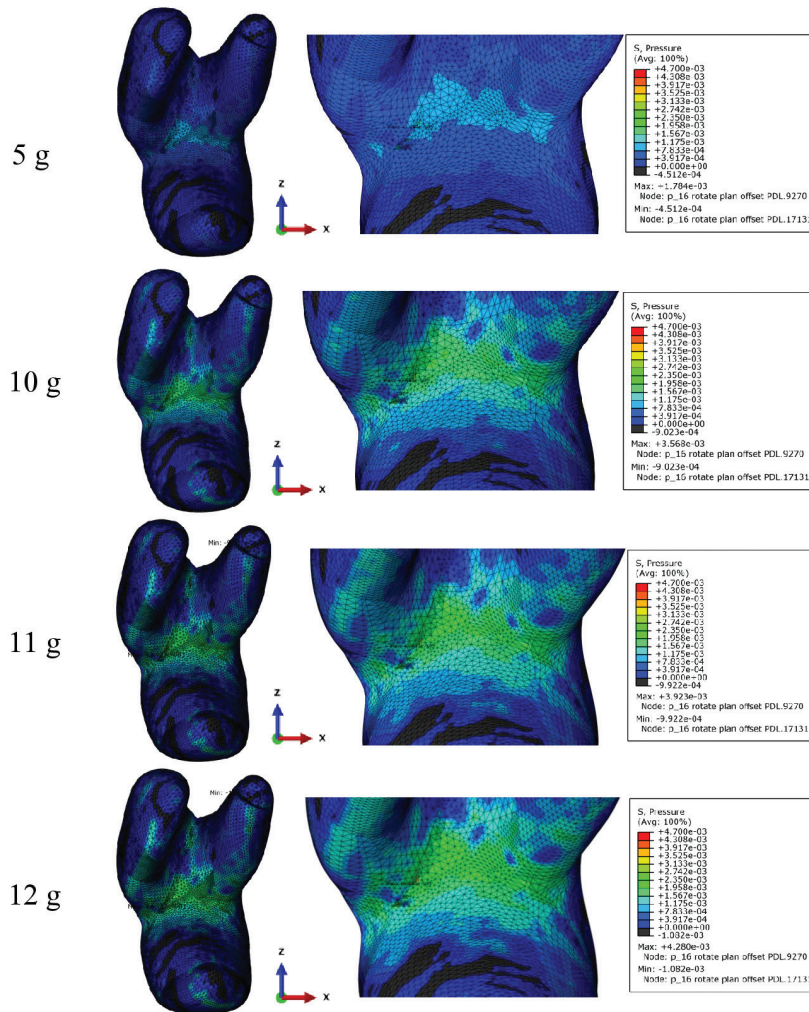
Results

First research hypothesis

In this study, the hydrostatic pressure (p) on the periodontal ligament of the maxillary first molar tooth, which is equal to $\sigma_H = (\sigma_1 + \sigma_2 + \sigma_3)/3$ with hydrostatic stress σ_H and the principal stresses σ_1 , σ_2 and σ_3 , was calculated. Hydrostatic pressure distributions (color-coded map) along the periodontal ligament of the maxillary first molar tooth when various force magnitudes were applied are shown in Figure 4. In the figure, the colors show the hydrostatic pressure values from 0.00 to 0.0047 MPa. Light grey color

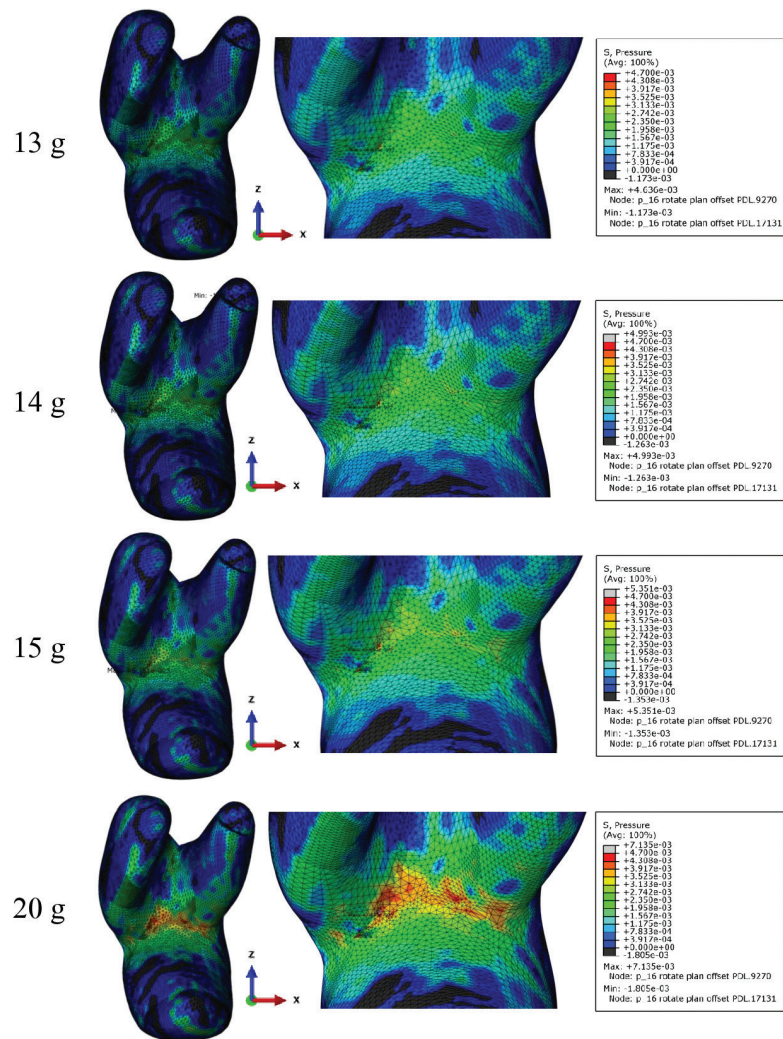
represents the areas in which hydrostatic pressure values were greater than 0.0047 MPa, whereas dark grey color represents the areas in which hydrostatic pressure values were less than zero. For the intrusive forces of 5, 10, 11, 12 and 13 g, there were no areas in which the hydrostatic pressure exceeded the periodontal capillary-vessel blood pressure of 0.0047 MPa. When an intrusive force of 14 g was applied, a small area in which the hydrostatic pressure exceeded the periodontal capillary-vessel blood pressure was found in the furcation region of the periodontal ligament of the maxillary first molar tooth (node 9270). Moreover, the

greater the force magnitude applied, the larger the area in which the hydrostatic pressure exceeded the periodontal capillary-vessel blood pressure. Furthermore, for intrusive forces of 14, 15, 20 and 25 g, areas in which the hydrostatic pressure exceeded the periodontal capillary-vessel blood pressure of 0.0047 MPa were found only in the furcation regions of the periodontal ligament of the maxillary first molar tooth. Periapical regions in which the hydrostatic pressure exceeded the periodontal capillary-vessel blood pressure were found when intrusive forces of 50 and 100 g were applied.



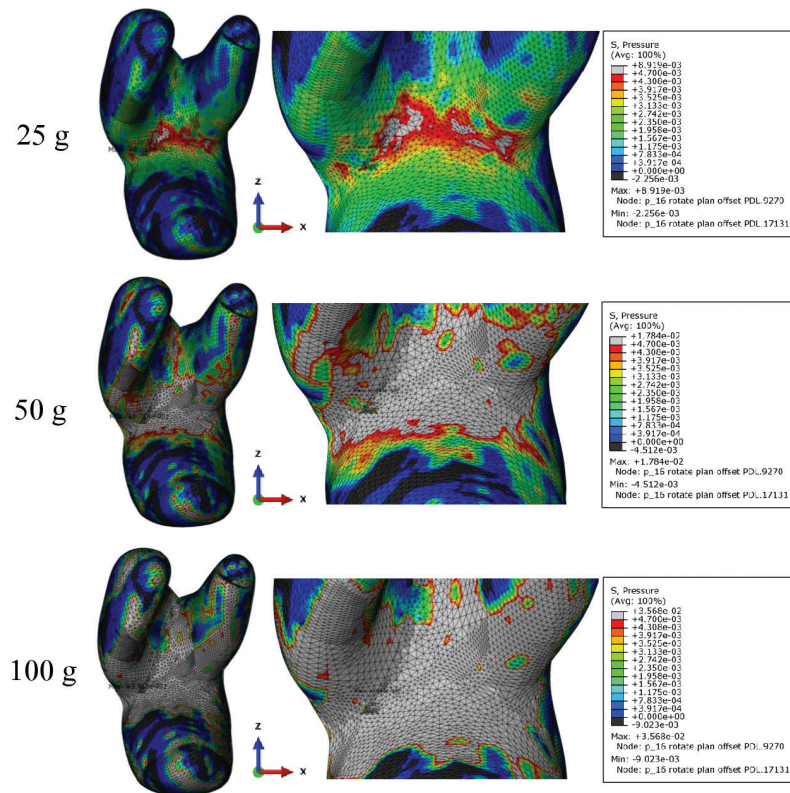
รูปที่ 4 ความดันหลอดเลือดฝอยในเอ็นยึดปริทันต์ของฟันกรามแท้บนซี่ที่หนึ่งเมื่อให้แรงในปริมาณต่าง ๆ กัน

Figure 4 Hydrostatic pressure distribution along the periodontal ligament of the maxillary first molar tooth when various force magnitudes (5, 10, 11, 12, 13, 14, 15, 20, 25, 50, and 100g) were applied.



รูปที่ 4 (ต่อ) ความดันหลอดเลือดฝอยในเอ็นยึดปริทันต์ของฟันกรามแท้บนซี่ที่หนึ่งเมื่อให้แรงในปริมาณต่าง ๆ กัน

Figure 4 (cont'd) Hydrostatic pressure distribution along the periodontal ligament of the maxillary first molar tooth when various force magnitudes (5, 10, 11, 12, 13, 14, 15, 20, 25, 50, and 100g) were applied.

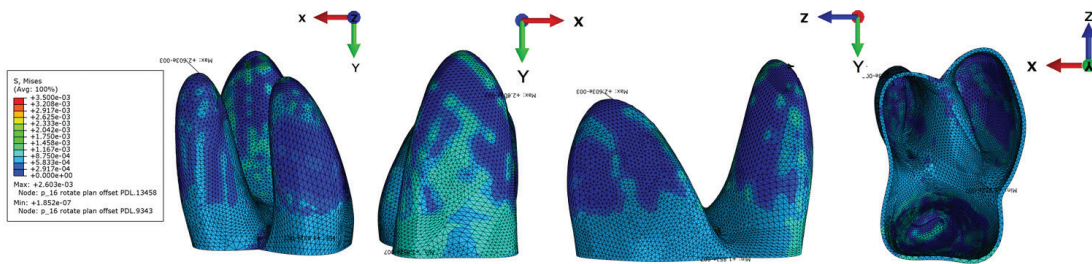


รูปที่ 4 (ต่อ) ความดันตลอดเลือดฝอยในเอ็นยึดปริทันต์ของฟันกรามแท้บนซี่ที่หนึ่งเมื่อให้แรงในปริมาณต่าง ๆ กัน
Figure 4 (cont'd) Hydrostatic pressure distribution along the periodontal ligament of the maxillary first molar tooth when various force magnitudes (5, 10, 11, 12, 13, 14, 15, 20, 25, 50, and 100g) were applied.

Second research hypothesis

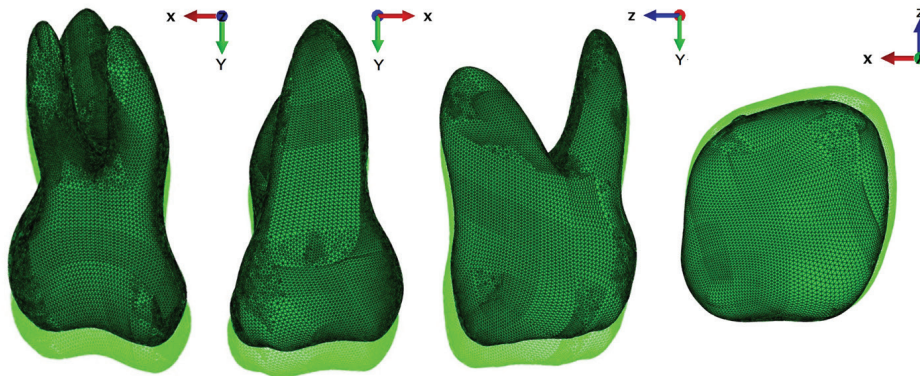
In the pattern of intrusion using two mini-screws, the stress distribution pattern on the periodontal ligament of the maxillary first molar tooth is shown in Figure 5. The maximum von Mises stress value was 0.002603 MPa at the apical third of the palatal side of the disto-buccal periodontal ligament. The standard deviation of von Mises stresses was 0.000314. Initial displacement of the maxillary first molar crown and root is shown in Table 3 and Figure 6.

In the pattern of intrusion using three mini-screws, the stress distribution is shown in Figure 7. The maximum von Mises stress value was 0.003187 MPa at the apical third of the buccal side of the palatal periodontal ligament. Overall, the palatal side of the periodontal ligament presented a more extended compressive region than did the buccal side. The standard deviation of von Mises stresses was 0.000392. Initial displacement of the first molar crown and root is shown in Table 4 and Figure 8.



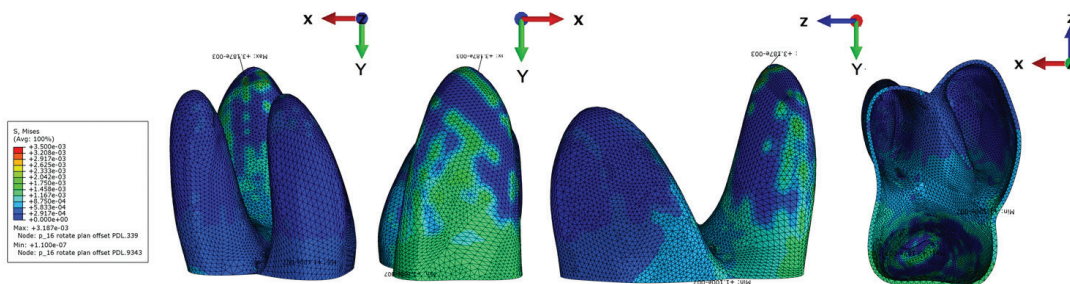
รูปที่ 5 การกระจายความเค้นในเอ็นยึดปริทันต์ของฟันกรามแท้บนซี่ที่หนึ่งเมื่อให้แรงกระทำสองแนวแรง

Figure 5 Von Mises stress distribution (color-coded map) along the periodontal ligament of the maxillary first molar when two intrusive forces were applied



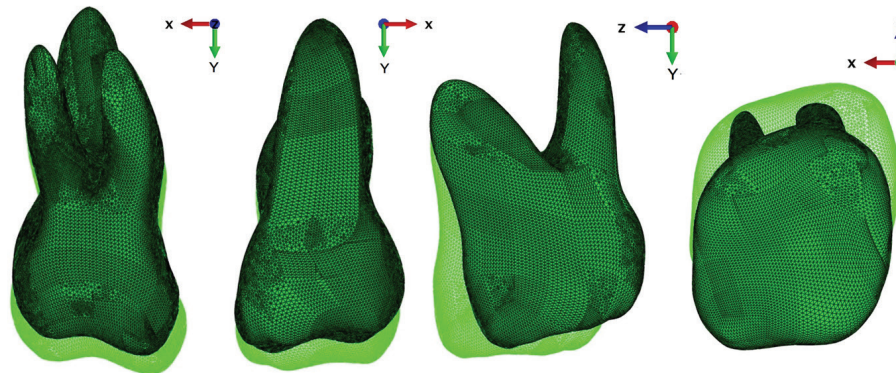
รูปที่ 6 ลักษณะการเคลื่อนที่เริ่มต้นและการซ้อนทับของฟันกรามแท้บนซี่ที่หนึ่งเมื่อให้แรงกระทำสองแนวแรง (สีเขียวอ่อนแสดงถึงตำแหน่งฟันก่อนการให้แรง, สีเขียวเข้มแสดงถึงตำแหน่งของฟันหลังการให้แรง)

Figure 6 Initial displacement and superimposition of the maxillary first molar tooth when two intrusive forces were applied (Bright green, before; Dark green, after).



รูปที่ 7 การกระจายความเค้นในเอ็นยึดปริทันต์ของฟันกรามแท้บนซี่ที่หนึ่งเมื่อให้แรงกระทำสามแนวแรง

Figure 7 Von Mises stress distribution (color-coded map) along the periodontal ligament of the maxillary first molar tooth when three intrusive forces were applied.



รูปที่ 8 ลักษณะการเคลื่อนที่เริ่มต้นและการซ้อนทับของฟันกรามแท้บนซี่ที่หนึ่งเมื่อให้แรงกระทำสามแนวแรง (สีเขียวอ่อนแสดงถึงตำแหน่งฟันก่อนการให้แรง, สีเขียวเข้มแสดงถึงตำแหน่งของฟันหลังการให้แรง)

Figure 8 Initial displacement and superimposition of the maxillary first molar tooth when three intrusive forces were applied (Bright green, before; Dark green, after).

ตารางที่ 3 ระยะการเคลื่อนที่เริ่มต้นตัวฟันและรากฟันของฟันกรามแท้บนซี่ที่หนึ่ง (มิลลิเมตร) เมื่อให้แรงกระทำสองแนวแรง โดยกำหนดให้ MBC หมายถึง ปุ่มฟันด้านแก้มใกล้กลาง, DBC หมายถึง ปุ่มฟันด้านแก้มไกลกลาง, MPC หมายถึง ปุ่มฟันด้านเพดานใกล้กลาง, DPC หมายถึง ปุ่มฟันด้านเพดานไกลกลาง, MBRA หมายถึง ปลายรากฟันด้านแก้มใกล้กลาง, DBRA หมายถึง ปลายรากฟันด้านแก้มไกลกลาง, PRA หมายถึง ปลายรากฟันด้านเพดาน นอกจากนี้ ระนาบ X หมายถึง ทิศทางด้านไกลกลาง ระนาบ Y หมายถึง ทิศทางด้านบดเคี้ยว และ ระนาบ Z หมายถึง ทิศทางด้านแก้ม

Table 3 Initial displacement of the maxillary first molar crown and root (mm) when two intrusive forces were applied. MBC, mesio-buccal cusp; DBC, disto-buccal cusp; MPC, mesio-palatal cusp; DPC, disto-palatal cusp; MBRA, mesio-buccal root apex; DBRA, disto-buccal root apex; PRA, palatal root apex; x-axis, distal direction; y-axis occlusal direction; z-axis, buccal direction.

Tooth	Part	Position	Displacement (mm)		
			ΔX	ΔY	ΔZ
Maxillary first molar tooth	Crown	MBC	1.8366E-04	-1.64515E-03	-9.76464E-04
		DBC	2.10976E-04	-1.82105E-03	-7.31094E-04
		MPC	4.26263E-04	-2.17517E-03	-9.26768E-04
		DPC	4.54999E-04	-2.34064E-03	-7.04652E-04
	Root	MBRA	-1.25788E-04	-1.63943E-03	3.42994E-04
		DBRA	-1.21652E-04	-1.70384E-03	4.89181E-04
		PRA	1.3788E-04	-2.30126E-03	5.41792E-04

ตารางที่ 4 ระยะการเคลื่อนที่เริ่มต้นตัวฟันและรากฟันของฟันกรามแท้บนซี่ที่หนึ่ง (มิลลิเมตร) เมื่อให้แรงกระทำสามแนวแรง โดยกำหนดให้ MBC หมายถึง ปุ่มฟันด้านแก้มใกล้กลาง, DBC หมายถึง ปุ่มฟันด้านแก้มไกลกลาง, MPC หมายถึง ปุ่มฟันด้านเพดานใกล้กลาง, DPC หมายถึง ปุ่มฟันด้านเพดานไกลกลาง, MBRA หมายถึง ปลายรากฟันด้านแก้มใกล้กลาง, DBRA หมายถึง ปลายรากฟันด้านแก้มไกลกลาง, PRA หมายถึง ปลายรากฟันด้านเพดาน นอกจากนี้ ระนาบ X หมายถึง ทิศทางด้านไกลกลาง ระนาบ Y หมายถึง ทิศทางด้านบดเคี้ยว และ ระนาบ Z หมายถึง ทิศทางด้านแก้ม

Table 4 Initial displacement of the maxillary first molar crown and root (mm) when three intrusive forces were applied. MBC, mesio-buccal cusp; DBC, disto-buccal cusp; MPC, meio-palatal cusp; DPC, disto-palatal cusp; MBRA, mesio-buccal root apex; DBRA, disto-buccal root apex; PRA, palatal root apex; x-axis, distal direction; y-axis occlusal direction; z-axis, buccal direction.

Tooth	Part	Position	Displacement (mm)		
			ΔX	ΔY	ΔZ
Maxillary first molar tooth	Crown	MBC	3.32192E-04	-6.0149E-04	-3.79807E-03
		DBC	2.90146E-04	-1.0621E-03	-3.79254E-03
		MPC	1.43077E-04	-2.6958E-03	-3.76671E-03
		DPC	1.14974E-04	-2.9869E-03	-3.73827E-03
	Root	MBRA	5.22758E-05	-5.08705E-04	9.28315E-04
		DBRA	5.09827E-05	-5.77913E-04	8.91798E-04
		PRA	-2.07342E-04	-3.03066E-03	1.50598E-03

Discussion

The accuracy of results depends on the accuracy of the finite element model, including the anatomy of the solid model, and of the material properties and the boundary conditions.⁽²⁸⁾ Even though a linear elastic model is generally used for the PDL, it is commonly accepted that the PDL component is nonlinear. In addition, previous investigations^(29,30) have proved that the transient characteristics of the PDL are more suitable for nonlinear constitutive models to describe the mechanical properties of the PDL. Several constitutive models have been proposed to characterize the hyperelasticity of the PDL.^(31,32) Therefore, the hyperelastic property of the PDL was taken into consideration in this investigation. Another parameter affecting the precision of the finite element analysis is the number of elements and nodes comprising the models. Consequently, in our study, we used elements as small as 0.2 mm to enhance the number of nodes in the critical regions where stress and displacement were

evaluated. Moreover, convergence tests of the finite element method models were completed.

To avoid root resorption, optimal intrusive force magnitude should be considered.⁽³³⁾ There is no current agreement in the literature about the optimal force to be used for molar intrusion. Some authors^(3,4,34) advise forces ranging from 30 to 100 g, whereas others suggest greater force magnitudes ranging from 150 to 500 g.^(5,6) In 2007, Hohmann *et al.*⁽³⁵⁾ suggested that hydrostatic pressure is one of the indicators of the regions in which root resorption can occur. Therefore, our study used this suggestion to identify the greatest force magnitude for maxillary first molar intrusion, using the finite element method. We found that the greatest magnitude of force, that can be applied to initiate the intrusion of maxillary first molar teeth without exceeding the periodontal capillary-vessel blood pressure, was 13 g. This force magnitude was much lower than that in previous studies. One reason might be that measuring

the amount of root resorption in most human studies^(3,6,10,36) was based on two-dimensional images (e.g., cephalometric films, periapical films and panoramic films), which frequently underestimate the extent of damage. Since resorptive areas can be extensive, shallow lacunae are not visible on radiographs.⁽³⁷⁾ There has been only one study⁽³⁸⁾ that focused on root resorption following molar intrusion using cone beam computed tomography (CBCT). Furthermore, 150 g of force was applied in that study. To date, there have been no clinical studies, using CBCT, and measuring the amount of root resorption following molar intrusion with a lighter force than 150 g. Another reason might be that the contacts between the maxillary second premolar, maxillary first molar and maxillary second molar teeth were defined as frictionless surfaces. Consequently, the greatest magnitude of force in this study may be lower than that in realistic situations.

Ramirez-Echave *et al.*⁽³⁹⁾ reported in their beagle dog study that light, constant, intrusive forces of between 50 and 200 g showed no significant differences in the amount of resorption produced. A human study by Owman-Moll *et al.*⁽⁴⁰⁾ also showed large individual variations in root resorption, independently of force magnitude. In contrast to the results of those studies, we found that the greater the force magnitude applied, the larger the area in which the hydrostatic pressure exceeded the periodontal capillary-vessel blood pressure. This meant that there were larger areas with high risk of root resorption. However, studies by Dellinger⁽⁴¹⁾ and Gonzales *et al.*⁽⁴²⁾ support our results. Dellinger reported in his monkey study that light forces (10-50 g) resulted in only slight root resorption, whereas a 100 g-force induced a greater amount of root resorption. Moreover, unacceptable, severe root resorption was found when a 300-g force was applied. These findings agree with those of a rat study by

Gonzales *et al.*, who found that light, 10-g forces applied to maxillary first molar teeth produced more tooth movement and less root resorption than did 25-, 50-, or 100-g forces.

Our study found that the furcations and root apices had more areas in which the hydrostatic pressure exceeded the periodontal capillary-vessel blood pressure than did regions other than furcations. This finding is in agreement with the results of previous studies.^(37,39,41,43) Firstly, when a 14-g force was applied, areas in which the hydrostatic pressure exceeded the periodontal capillary-vessel blood pressure were found only in the furcation. Then, the areas in which the hydrostatic pressure exceeded the periodontal capillary-vessel blood pressure were larger when heavier forces were applied. When a 50-g force was applied, areas in which the hydrostatic pressure exceeded the periodontal capillary-vessel blood pressure were found in the furcation and root apices. A possible explanation for the more extensive areas in which the hydrostatic pressure exceeded the periodontal capillary-vessel pressure in the furcation and apical regions as compared to other regions may be that bone and root morphology might be factors that affect the hydrostatic pressure in the region of the PDL, since the furcation and apical regions have more areas that are perpendicular to intrusive forces.^(37,39,41)

Although, the hydrostatic pressure is one of the indicators of the regions in which root resorption can occur, the amount of root resorption cannot be predicted from only the hydrostatic pressure, because various factors are related to root resorption during orthodontic treatment, such as cementum thickness,⁽³⁹⁾ type of cementum (cellular vs acellular cementum),⁽³⁷⁾ treatment time,⁽⁴⁴⁾ Age,⁽⁴⁴⁾ and bone thickness.⁽⁴⁴⁾

In the first research hypothesis, the intrusive force was applied parallel to the long axis of the tooth at the middle of the occlusal surface of the maxillary first

molar tooth. This direction of force cannot be applied in orthodontics applications. Therefore, further studies are needed to evaluate the magnitude of force in a direction that can be clinically used.

Nowadays, there are many patterns for maxillary molars intrusion anchored in mini-screws.^(3,12,14,16,45-47) However, there is no agreement about the ideal number of mini-screws to be inserted or the optimal pattern to intrude maxillary first molar teeth with maximum efficiency. In our study, we chose two patterns that are often recommended and referred to by many authors.^(12,14,47)

The stress values of the maxillary first molar tooth were compared between these two patterns of intrusion. The maximum von Mises stress value in the pattern of intrusion using three mini-screws was greater than that in the pattern of intrusion using two mini-screws. Increased stress values were observed at the palatal side of the periodontal ligament. Moreover, the standard deviation of von Mises stress in the pattern of intrusion using three mini-screws was higher than that in the pattern of intrusion using two mini-screws. Therefore, the pattern with three mini-screws had a greater risk for root resorption than that with two mini-screws.

The amount of intrusive movement of the maxillary first molar in the pattern of intrusion using three mini-screws was less than that in the pattern of intrusion using two mini-screws. In addition, the amount of palatal tipping movement of the first molar in the pattern of intrusion using three mini-screws was more than that in the pattern of intrusion using two mini-screws. Consequently, our study suggests that the pattern with two mini-screws was the optimal pattern of force for intrusion of maxillary first molar teeth because the more balanced intrusion was identified in this pattern. The pattern with two mini-screws provided more bodily movement than that with three mini-screws and this type of movement is favorable in orthodontics.

Furthermore, three mini-screws for maxillary first molar intrusion would be too much for a patient.

Even though the design of both patterns was intended to control the buccopalatal position of the tooth during intrusion, palatal tipping was found in both patterns. Variations in tooth morphologies and root angles, inclination differences of the vestibular and palatal slopes of the alveolar bone and the palatal depth can affect the stress distribution and the path of the intrusion movement. In the pattern of intrusion using two mini-screws, the palatal and buccal force vectors were angulated 24 and 15 degrees, respectively, to the long axis of the maxillary first molar tooth. However, in the pattern of intrusion using three mini-screws, the palatal force vector was angulated 45 degrees to the long axis of the maxillary first molar tooth, whereas the two buccal force vectors were angulated 15 degrees. Since the palatal angle of 24 degrees was little larger than the buccal angle of 15 degrees, only little palatal tipping was found in the pattern using three mini-screws. Because the palatal angle of 45 degrees was larger than the buccal angle of 15 degrees, more palatal tipping was found in the pattern using three mini-screws. Therefore, besides considering the balanced magnitude of forces, the balanced direction of force should be considered as well. Moreover, because of individual variations, it is essential to use unique mechanics and force systems for each patient.

In our study, static finite element analysis simulated only the initial tooth movement in the maxillary first molar teeth and the initial stress distribution along the periodontal ligament. The initial movement may be different from the orthodontic movement. This difference is due to a change in the force system and biologic response during the tooth movement. In addition, other forces act continually on

the maxillary first molar teeth from the cheek, the tongue, and the mandibular teeth. The direction and amount of these forces are undefined, and their effects on orthodontic movement are unclear. Accordingly, these forces are not considered in the simulation study.

Another limitation of this study was the assumption that the periodontal ligament and bone were homogeneous, isotropic and uniform in thickness. These limitations can cause differences between simulation studies and clinical applications.

Conclusions

The magnitude of force that can be applied to initiate the intrusion of maxillary first molar teeth without exceeding the periodontal capillary-vessel blood pressure, was 13 g. Moreover, these results suggest that the furcation region of the maxillary first molar teeth should be considered to be prone to resorption earlier than any other region during maxillary first molar intrusion treatment.

Since the pattern with two mini-screws provided more bodily movement than that with three mini-screws, it was concluded that the optimal pattern of force for the intrusion of the maxillary first molar was the pattern with two mini-screws.

Acknowledgements

We would like to express our appreciation to Dr. M. Kevin O Carroll, Professor Emeritus of the University of Mississippi School of Dentistry, USA, and Faculty Consultant at Chiang Mai University, Faculty of Dentistry, for his assistance in the preparation of the manuscript and to Department of Orthodontics and Pediatric Dentistry, Chiang Mai University, for the support in financial aid of this research.

References

1. Eliades T, Gioka C. Orthodontic dental intrusion: indications, histological changes, biomechanical principles and possible side effects. *Helv Orthod Rev* 2003; 6: 129-146.
2. Proffit W, Fields H, Sarver D. *Contemporary orthodontics* 5th ed. St. Louis: Mosby; 2013: 296.
3. Heravi F, Bayani S, Madani AS, Radvar M, Anbiaee N. Intrusion of supra-erupted molars using miniscrews: Clinical success and root resorption. *Am J Orthod Dentofacial Orthop* 2001; 139(4): S170-S175.
4. Carrillo R, Rossouw PE, Franco PF, Opperman LA, Buschang PH. Intrusion of multiradicular teeth and related root resorption with mini-screw implant anchorage: A radiographic evaluation. *Am J Orthod Dentofacial Orthop* 2007; 132(5): 647-655.
5. Park Y, Lee S, Kim D, Jee S. Intrusion of posterior teeth using mini-screw implants. *Am J Orthod Dentofacial Orthop* 2003; 123: 690-694.
6. Umemori M, Sugawara J, Mitani H, Nagasaka H, Kawamura H. Skeletal anchorage system for open-bite correction. *Am J Orthod Dentofacial Orthop* 1999; 115(2): 166-174.
7. Ersahan S, Sabuncuoglu FA. Effects of magnitude of intrusive force on pulpal blood flow in maxillary molars. *Am J Orthod Dentofacial Orthop* 2015; 148(1): 83-89.
8. Drenker E. Calculating continuous archwire forces. *Angle Orthod* 1988; 58(1): 59-70.
9. Greenfield RL. Simultaneous torquing and intrusion auxiliary. *J Clin Orthod* 1993; 27(6): 305-318.
10. Erverdi N, Keles A, Nanda R. The Use of skeletal anchorage in open bite treatment: A cephalometric evaluation. *Angle Orthod* 2004; 74(3): 381-390.
11. Chang YJ, Wu CB, Wu HY, Kok SH, Chang HF, Chen YJ. Miniscrew anchorage for molar intrusion. *J Clin Orthod* 2004; 38: 300-325.

12. Kravitz ND, Kusnoto B, Tsay TP, Hohlt WF. The use of temporary anchorage devices for molar intrusion. *J Am Dent Assoc* 2007; 138(1): 56-64.
13. Lee JS. *Applications of orthodontic mini-implants* 1st ed. Chicago:Quintessence; 2007.
14. Lin JC, Liou EJ, Yeh CL. Intrusion of overerupted maxillary molars with miniscrew anchorage. *J Clin Orthod* 2006; 40(6): 378-383.
15. Telma MA, Mauro HAN, Fernanda CMF, Marcos AVB. Tooth intrusion using mini-implants. *Dental Press J Orthod* 2008; 13(5): 36-48.
16. Yao CC, Lee JJ, Chen HY, Chang ZC, Chang HF, Chen YJ. Maxillary molar intrusion with fixed appliances and mini-implant anchorage studied in three dimensions. *Angle Orthod* 2005; 75(5): 754-760.
17. Rubin C, Krishnamurthy N, Capilouto E, Yi H. Stress analysis of the human tooth using a three-dimensional finite element model. *J Dent Res* 1983; 62: 82-86.
18. Schwarz AM. Tissue changes incident to orthodontic tooth movement. *Int J Dent Clin* 1932; 18: 331-352.
19. Deetjen P, Speckmann EJ. *Physiologie* 5th ed. Baltimore: Elsevier; 1994.
20. Wheeler RC. *A textbook of dental anatomy and physiology* 2nd ed. Philadelphia: Saunders; 1950.
21. Coolidge ED. The Thickness of the Human Periodontal Membrane. *J Am Dent Assoc Dent Cosmos* 1937; 24(8): 1260-1270.
22. Tanne K, Sakuda M, Burstone CJ. Three-dimensional finite element analysis for stress in the periodontal tissue by orthodontic forces. *Am J Orthod Dentofacial Orthop* 1987; 92(6): 499-505.
23. Yoshida N, Koga Y, Peng CL, Tanaka E, Kobayashi K. In vivo measurement of the elastic modulus of the human periodontal ligament. *Med Eng Phys* 2001; 23(8): 567-572.
24. lixiang Z, Huang H, Tang W, Yan B, Wu B. International conference on advances in computational modeling and simulation mechanical responses of periodontal ligament under a realistic orthodontic loading. *Procedia Eng* 2012; 31: 828-833.
25. Lee KJ, Joo E, Kim KD, Lee JS, Park YC, Yu HS. Computed tomographic analysis of tooth-bearing alveolar bone for orthodontic miniscrew placement. *Am J Orthod Dentofacial Orthop* 2009; 135(4): 486-494.
26. Garib DG, Yatabe MS, Ozawa TO, Silva Filho OGd. Alveolar bone morphology under the perspective of the computed tomography: Defining the biological limits of tooth movement. *Dental Press J Orthod* 2010; 15: 192-205.
27. Mohammed N, Noor FKA, Ata'a G. Palatal dimensions in different occlusal relationships. *J Bagh Coll Dentistry* 2012; 24(1): 116-120.
28. Cattaneo PM, Dalstra M, Melsen B. The Finite Element Method: a Tool to Study Orthodontic Tooth Movement. *J Dent Res* 2005; 84(5): 428-433.
29. Pietrzak G, Curnier A, Botsis J, Scherrer S, Wiskott A, Belser U. A nonlinear elastic model of the periodontal ligament and its numerical calibration for the study of tooth mobility. *Comput Methods Biomech Biomed Engin* 2002; 5(2): 91-100.
30. Toms SR, Eberhardt AW. A nonlinear finite element analysis of the periodontal ligament under orthodontic tooth loading. *Am J Orthod Dentofacial Orthop* 2003; 123(6): 657-665.
31. Natali AN, Pavan PG, Scarpa C. Numerical analysis of tooth mobility: formulation of a non-linear constitutive law for the periodontal ligament. *Dent Mater J* 2004; 20(7): 623-629.

32. Qian L, Todo M, Morita Y, Matsushita Y, Koyano K. Deformation analysis of the periodontium considering the viscoelasticity of the periodontal ligament. *Dent Mater J* 2009; 25(10): 1285-1292.
33. Burstone CR. Deep overbite correction by intrusion. *Am J Orthod* 1977; 72(1): 1-22.
34. Tasanapanont J, Wattanachai T, Apisariyakul J, Pothacharoen P, Ongchai S, Kongtawelert P, et al. Biochemical and clinical assessments of segmental maxillary posterior tooth intrusion. *Int J Dent* [Article ID 2689642]. 2017 Feb;2017:[about7p.]. Available from: HYPERLINK<http://doi.org/10.1155/2017/2689642> <http://doi.org/10.1155/2017/2689642>
35. Hohmann A, Wolfram U, Geiger M, Boryor A, Sander C, Faltin R, et al. Periodontal ligament hydrostatic pressure with areas of root resorption after application of a continuous torque moment. *Angle Orthod* 2007; 77(4): 653-659.
36. Ari-Demirkaya A, Masry MA, Erverdi N. Apical root resorption of maxillary first molars after intrusion with zygomatic skeletal anchorage. *Angle Orthod* 2005; 75(5): 761-767.
37. Ohmae M, Saito S, Morohashi T, Seki K, Qu H, Kanomi R, et al. A clinical and histological evaluation of titanium mini-implants as anchors for orthodontic intrusion in the beagle dog. *Am J Orthod Dentofacial Orthop* 2001; 119(5): 489-497.
38. Li W, Chen F, Zhang F, Ding W, Ye Q, Shi J, et al. Volumetric measurement of root resorption following molar mini-crew implant intrusion using cone beam computed tomography. *PLoS One* 2013; 8(4): e60962.
39. Ramirez-Echave JI, Buschang PH, Carrillo R, Rossouw PE, Nagy WW, Opperman LA. Histologic evaluation of root response to intrusion in mandibular teeth in beagle dogs. *Am J Orthod Dentofacial Orthop* 2011; 139(1): 60-69.
40. Owman-Moll P, Kurol J, Lundgren D. The effects of a four-fold increased orthodontic force magnitude on tooth movement and root resorptions. An intra-individual study in adolescents. *Eur J Orthod* 1996; 18(3): 287-294.
41. Dellinger EL. A histologic and cephalometric investigation of premolar intrusion in the *Macaca speciosa* monkey. *Am J Orthod* 1967; 53(5): 325-355.
42. Gonzales C, Hotokezaka H, Yoshimatsu M, Yozgatian JH, Darendeliler MA, Yoshida N. Force magnitude and duration effects on amount of tooth movement and root resorption in the rat molar. *Angle Orthod* 2008; 78(3): 502-509.
43. Bondevik O. Tissue changes in the rat molar periodontium following application of intrusive forces. *Eur J Orthod* 1980; 2(1): 41-49.
44. Picanço GV, Freitas KMSd, Cançado RH, Valarelli FP, Picanço PRB, Feijão CP. Predisposing factors to severe external root resorption associated to orthodontic treatment. *Dental Press J Orthod* 2013; 18: 110-120.
45. Grenga V, Bovi M. Corticotomy-enhanced intrusion of an overerupted molar using skeletal anchorage and ultrasonic surgery. *J Clin Orthod* 2013; 47(1): 50-55.
46. Xun C, Zeng X, Wang X. Microscrew anchorage in skeletal anterior open-bite treatment. *The Angle Orthodontist* 2007; 77(1): 47-56.
47. Paccini JVC, Cotrim-Ferreira FA, Ferreira FV, Freitas KMSd, Cançado RH, Valarelli FP. Efficiency of two protocols for maxillary molar intrusion with mini-implants. *Dental Press J Orthod* 2016; 21: 56-66.

